ResearchGate

See discussions, stats, and author profiles for this publication at: https://www.researchgate.net/publication/9073222

Epicardium is required for the full rate of myocyte proliferation and levels of expression of myocyte mitogenic factors FGF2 and its receptor, FGFR-1, but not for transmural myocar...

ARTICLE *in* DEVELOPMENTAL DYNAMICS · OCTOBER 2003

Impact Factor: 2.38 · DOI: 10.1002/dvdy.10360 · Source: PubMed

CITATIONS
60

READS
122

3 AUTHORS, INCLUDING:

Victoria Ballard
GlaxoSmithKline plc.
18 PUBLICATIONS **347** CITATIONS

SEE PROFILE

Available from: Victoria Ballard
Retrieved on: 25 January 2016

DEVELOPMENTAL DYNAMICS 228:161–172, 2003

ARTICLE

Epicardium Is Required for the Full Rate of Myocyte Proliferation and Levels of Expression of Myocyte Mitogenic Factors FGF2 and Its Receptor, FGFR-1, but not for Transmural Myocardial Patterning in the Embryonic Chick Heart

David J. Pennisi, Victoria L.T. Ballard, and Takashi Mikawa*

**Proper heart development requires patterning across the myocardial wall. Early myocardial patterning is characterized by a transmural subdivision of the myocardium into an outer, highly mitotic, compact zone and an inner, trabecular zone with lower mitotic activity. We have shown previously that fibroblast growth factor receptor (FGFR) -mediated signaling is central to myocyte proliferation in the developing heart. Consistent with this, FGFR-1 and FGF2 are more highly expressed in myocytes of the compact zone. However, the mechanism that regulates the transmural pattern of myocyte proliferation and expression of these mitogenic factors is unknown. The present study examined whether this transmural patterning occurs in a myocardium-autonomous manner or by signals from the epicardium. Microsurgical inhibition of epicardium formation in the embryonic chick gives rise to a decrease in myocyte proliferation, accounting for a thinner compact myocardium. We show that the transmural pattern of myocyte mitotic activity is maintained in these hearts. Consistent with this, the expression patterns of FGF1, FGF2, and FGFR-1 across the myocardium persist in the absence of the epicardium. However, FGF2 and FGFR-1 mRNA levels are reduced in proportion to the depletion of epicardium. The results suggest that epicardium-derived signals are essential for maintenance of the correct amount of myocyte proliferation in the compact myocardium, by means of levels of mitogen expression in the myocardium. However, initiation and maintenance of transmural patterning of the myocardium occurs largely independently of the epicardium. *Developmental Dynamics 228:161–172, 2003.*
© 2003 Wiley-Liss, Inc.

Key words: Epicardium, myocardium, fibroblast growth factor receptor, chick embryo, heart development

Received 30 April 2003; Accepted 10 June 2003

INTRODUCTION

Heart development begins with formation of the primitive heart tube that consists of two epithelial layers, the outer myocardium and inner endocardium (Manasek, 1969a). Soon after the double-walled heart tube forms, the epicardium begins to envelop the heart, forming the outermost, epithelial layer (Ho and Shimada, 1978; Virágh and Challice, 1981; Hiruma and Hirakow, 1989). The epicardium also provides cells of the coronary vasculature and connective tissues of the heart (Mikawa and Fischman, 1992; Mikawa and Gourdie, 1996; Dettman et al., 1998; Pérez-Pomares et al., 1998; Li et al., 2002). In addition to these three layers, cardiac neural crest cells migrate to the heart and participate in cardiac patterning and remodeling, as well as differentiating into cardiac ganglia and great vessel smooth muscle (reviewed in Kirby, 1999).

As the heart tube forms, morphogenetic patterning of the myocar-

Department of Cell and Developmental Biology, Cornell University Medical College, New York, New York
Grant sponsor: NIH; Grant numbers: HL54128; HL62175; HL67150.
Drs. Pennisi and Ballard contributed equally to this work.
Dr. Ballard's current address is Department of Medicine, Cornell University Medical College, 1300 York Avenue, New York, NY, 10021.
*Correspondence to: Takashi Mikawa, Department of Cell and Developmental Biology, Cornell University Medical College, 1300 York Avenue, New York, NY 10021. E-mail: tmikaw@med.cornell.edu

DOI 10.1002/dvdy.10360

© 2003 Wiley-Liss, Inc.

dium becomes evident along the anteroposterior embryonic axis. This anteroposterior patterning is characterized by subdivision of the straight heart tube into the outflow tract, the presumptive ventricle, the presumptive atrium and inflow tract (reviewed in Fishman and Chien, 1997). Subsequent patterning along the dorsoventral and left–right axes of the heart governs its right-sided looping (reviewed in Männer, 2000). In addition to patterning along the three major embryonic axes, other morphogenetic patterning events take place along the transmural axis, i.e., across the myocardial wall from the epicardial to the endocardial side.

The myocardium can be divided into two subcomponents: the outermost region, the compact myocardium, consisting of myocytes that are epithelioid and highly mitotic; and the inner, trabeculated myocardium that is less mitotically active (Manasek, 1968; Jeter and Cameron, 1971; Tokuyasu, 1990; Thompson et al., 1995). At this stage, the myocardial wall is avascular and is thought to be nourished by diffusion through the endocardium, by means of trabecular channels that markedly increase endocardial surface area (Rychter and Ostádal, 1971; Rychterova, 1971). Thus, the compact myocardium is essential for myocardial growth and the trabeculated myocardium is essential for myocardial survival. However, little is known about the mechanism(s) that regulates transmural subdivision of the myocardium into these two distinct compartments, and whether this regulation is achieved in a myocardium-autonomous manner or by means of paracrine induction.

Inductive signals from the adjacent tissue layers have been postulated to pattern the myocardium. Signals from the endocardium are necessary for trabeculation, which involve a paracrine interaction of Neuregulin and its receptor tyrosine kinases, erbB2 and erbB4 (Corfas et al., 1995; Meyer and Birchmeier, 1995; Kramer et al., 1996; Ford et al., 1999). Disruption of Neuregulin signaling results in embryonic lethality during gestation and hearts that display a striking lack of trabeculae but an apparently normal compact myocardium (Gassmann et al., 1995; Lee et al., 1995; Meyer and Birchmeier, 1995). These studies demonstrate the necessity of endocardium-derived signals for trabeculation, but do not explain how the compact zone is formed and maintained during myocardium development.

The involvement of the epicardium in myocardial patterning has also been suggested. Several animal models that lack an epicardium, such as VCAM-1 and α4 inte-

Fig. 1. Production of epicardium-deficient hearts in the chick embryo. **A:** Proepicardium (PE) outgrowth was inhibited by insertion of a piece of shell membrane (arrow) between the PE and the heart tube at Hamburger and Hamilton stages 16–17. **B:** Microsurgical manipulation to inhibit PE outgrowth in ovo. **C:** Higher magnification of inserted shell membrane (blue arrow) in situ. **D–K:** Whole-mount views of sham-operated and test-operated hearts at embryonic day (E) 6 and E8. Sham-operated heart at E6 (D) and E8 (H). Test-operated hearts are shown with varying degrees of dysmorphogenesis at E6 (E–G) and E8 (I–K). The most affected hearts appear on the right for each stage examined. **L–O:** Whole-mount cytokeratin immunostaining demonstrated successful inhibition of epicardium formation; cytokeratin immunostaining in a sham-operated heart (L) and test hearts (M–O) at E6. Note that varying degrees of epicardial inhibition were obtained. **P–S:** Cytokeratin section immunostaining confirms epicardium deficiency in test-operated hearts. Sections of a sham-operated heart at E6 (P) and a test heart at E6 (R) stained for cytokeratin protein. Q,S: Higher magnification views of the boxed areas in (P) and (R), respectively. Arrows indicate areas of epicardial covering (P,Q). Note the absence of the epicardium in the test heart shown (R,S). m, myocardium; pe, proepicardium; ot, outflow tract; lv, left ventricle; rv, right ventricle; ao, aorta.

Fig. 2. Epicardium-deficient hearts display a marked reduction in myocardial thickness and a slight increase in cell density. **A–H:** Hematoxylin and eosin staining of sections. A: embryonic day (E) 6 sham-operated heart. C: E6 epicardium-deficient heart. E: E8 sham-operated heart. G: E8 epicardium-deficient heart. B,D,F,H: Higher magnifications of the boxed areas in A, C, E, G, respectively. Note, the outermost myocytes of the myocardium of epicardium-deficient hearts remain more compact than inner myocytes. **I:** Quantification of the reduction in the thickness of the myocardial compact layer in epicardium-deficient hearts at E6 and E8. **J:** Quantification of the increased cell density in the myocardial compact layer of epicardium-deficient hearts at E6 and E8. At least three examples each of epicardium-deficient and sham-operated hearts were used for quantitative analysis at each stage examined. lv, left ventricle; rv, right ventricle; m, myocardium; epi, epicardium. Open bars, sham-operated; filled bars, epicardium-deficient. $*P < 0.1$; $**P < 0.05$; $***P < 0.005$. Scale bars = 200 μm in A,C,E,G, 20 μm in B,D,F,H.

Fig. 3. Terminal deoxynucleotidyl transferase-mediated biotinylated UTP nick end labeling (TUNEL) assays reveal an increase in the rate of apoptosis in cells of the myocardium in epicardium-deficient hearts. **A:** Section of the right ventricular wall of an embryonic day (E) 6 sham-operated heart. **C:** Section of the right ventricular wall of an E6 epicardium-deficient heart. **B,D:** Higher magnifications of the boxed areas in A and C, respectively. **E:** Quantitative analysis of TUNEL-positive cells in the myocardium of sham-operated hearts (open bars) and epicardium-deficient hearts (filled bars) at E6 (sham-operated, standard deviation from the mean (SDM), 0.75; epicardium-deficient, SDM, 2.13). **F:** Section of the right ventricular wall of an E8 sham-operated heart. **H:** Section of the right ventricular wall of an E8 epicardium-deficient heart. **G,I:** Higher magnification of the boxed areas in F and H, respectively. **J:** Quantitative analysis of the number of TUNEL-positive cells in the myocardium of sham-operated hearts (white bars) and epicardium-deficient hearts (black bars) at E8 (sham-operated, SDM, 4.17; epicardium-deficient, SDM, 32.8). $*P < 0.005$. Arrows, TUNEL-positive cells. m, myocardium; epi, epicardium. Scale bars = 50 μm in A,C,F,H, 20 μm in B,D,G,I.

Fig. 4. Epicardium-deficient hearts display a reduced myocyte clone size. **A:** Proepicardium outgrowth inhibition and tagging of individual myocytes of the heart tube at HH stages 16–17 (embryonic day (E) 3) with the retroviral vector CXL. Sham-operated **(B–D)** and epicardium-deficient hearts **(E–G)** at E7 after X-gal staining, showing areas of viral infection. Whole-mount views of a sham-operated heart at E7 (B) and an epicardium-deficient heart at E7 (E). C,F: Higher magnifications of the boxed areas in B and E, respectively. Sections showing X-gal–positive myocyte clones in a sham-operated heart at E7 (D) and an epicardium-deficient heart at E7 (G). **H:** Mean X-gal–positive myocyte clone size at E7 = 49 (sham-operated (Epi+), standard deviation from the mean (SDM), 13.8) and 29 (epicardium-deficient (Epi-), SDM, 13.0). $P < 0.015$. pe, proepicardium; m, myocardium; epi, epicardium. Arrows, X-gal–positive myocyte clones. Scale bars = 50 μm in D,G.

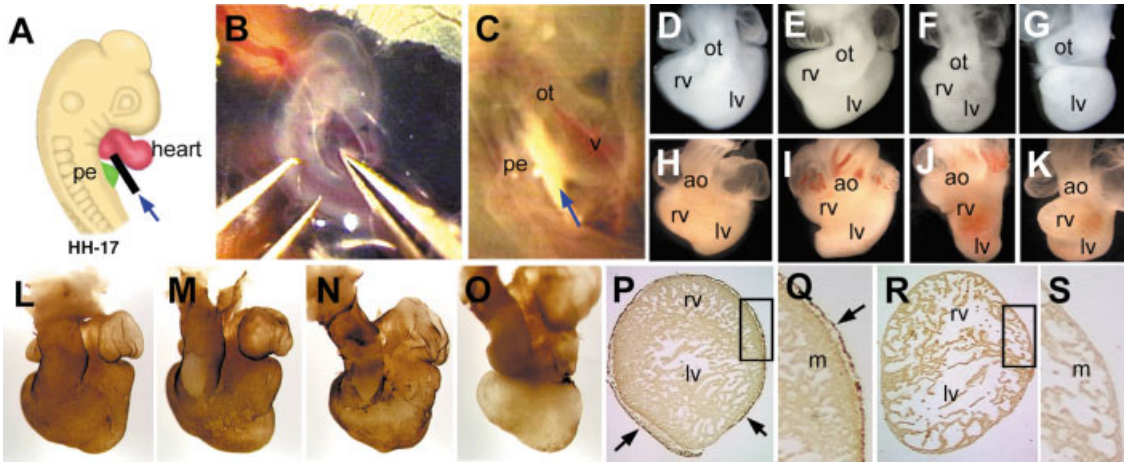

Fig. 1.

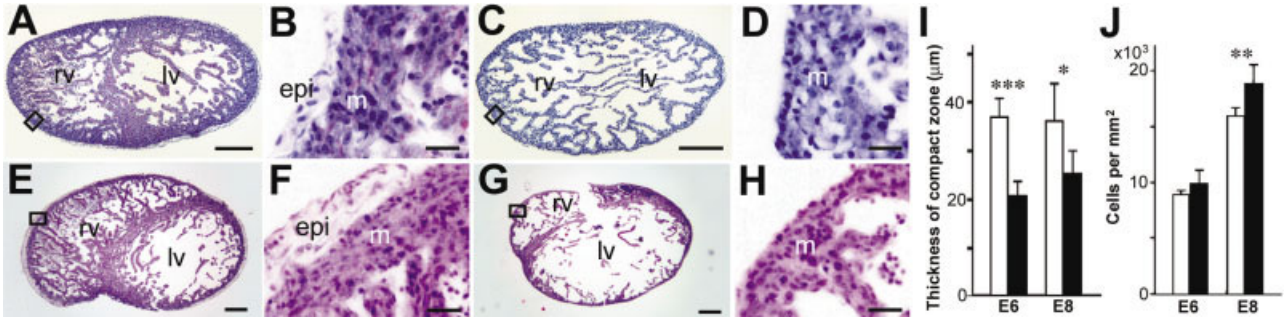

Fig. 2.

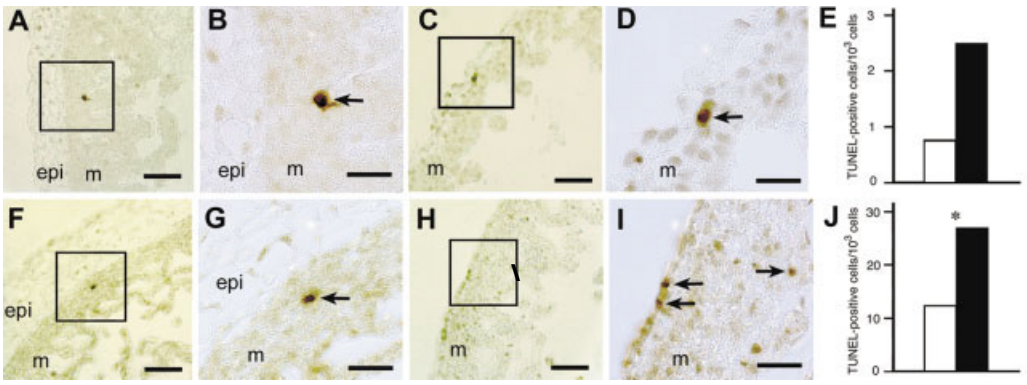

Fig. 3.

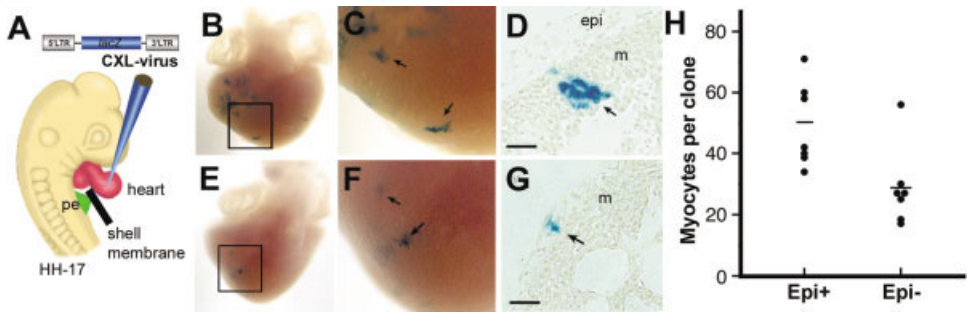

Fig. 4.

grin null mice, show a range of secondary cardiac abnormalities, including thinning of the myocardial wall, ventricular septal defects, and cardiac failure (Kwee et al., 1995; Yang et al., 1995). Retinoid signaling in the epicardium has also been implicated in myocardial development, with mice null for retinoid X receptor-α displaying aberrant or incomplete formation of the epicardium, as well as thinner ventricular walls and interventricular septa (Kastner et al., 1994; Sucov et al., 1994). These are similar to abnormalities observed in rodents deficient in vitamin A, the precursor of retinoic acid (Wilson and Warkany, 1949). Additionally, *Wilm's Tumor-1* knockout embryonic mice display a partial or incomplete formation of the epicardium concurrent with myocardial dysmorphogenesis, suggesting an interaction between these tissues (Kreidberg et al., 1993; Moore et al., 1999). The epicardium is further implicated in myocardial development by experiments in avian embryos where epicardium formation is inhibited by physical obstruction (Männer, 1993). A reduction in the thickness of the ventricular myocardium was observed as well as ventricular septal defects in epicardium-deficient hearts (Gittenberger-de Groot et al., 2000). However, it remains unclear whether the epicardium exerts this effect by means of regulation of growth, remodeling, or survival of cells in the compact myocardium.

Coincident with the morphogenetic patterning across the myocardium in the developing heart, a transmural gradient of expression of several myocyte-mitogenic factors, including fibroblast growth factor-2 (FGF2; Kardami and Fandrich, 1989; Consigli and Joseph-Silverstein, 1991; Cummins, 1993) and its corresponding receptors (FGFRs; Patstone et al., 1993), NT-3, trk-C (Lin et al., 2000), and TBX5 (Hatcher et al., 2001) have been detected. Of these mitogenic factors, it is known that FGFR-mediated signaling is essential for myocyte proliferation (Mikawa, 1995; Mima et al., 1995; Gisselbrecht et al., 1996; Ciruna et al., 1997; Sheikh et al., 1997, 1999; Michelson et al., 1998). FGF-2 and FGFR-1 expression is higher in the compact myocardium than the trabeculae, coincident with areas of high and low myocyte mitotic activity. It is unknown how the transmural gradient of FGF expression is initiated and maintained during heart development. Also unclear is whether expression of FGF-signaling components is regulated by signals from the epicardium.

To clarify these questions, the present study examined the embryonic chick heart for changes in proliferation, density, and survival of myocytes in the absence of epicardium. Additionally, expression patterns of FGF signaling components in the absence of the epicardium were examined to determine whether these are regulated by the epicardium. Microsurgical inhibition of epicardium formation gave rise to hearts that display a reduction in the thickness of the ventricular compact zone, consistent with previous studies. Importantly, despite the thinning of the compact myocardium in epicardium-deficient hearts, the transmural pattern of both myocyte proliferation and myocyte growth factors was initiated and maintained. However, the level of myocyte proliferation was slightly reduced in epicardium-deficient hearts. Consistent with this finding, FGF2 and FGFR-1 mRNA levels were reduced in epicardium-deficient hearts. This reduction was largely proportional to the extent of epicardial depletion. We conclude that the epicardium is necessary for maintaining the full rate of myocardial cell division and levels of expression of FGF signaling components, yet the myocardium can initiate and maintain the transmural pattern of growth factors and myocyte proliferation in an epicardium-independent manner.

RESULTS

Inhibition of Epicardium Formation

To examine the influence of the epicardium on myocardial patterning, epicardium-deficient hearts were produced by using a microsurgical protocol developed by Männer (1993). Insertion of a small piece of eggshell membrane between the proepicardium (PE) and the myocardium (Fig. 1A-C) at embryonic day (E) 3 resulted in hearts lacking an intact epicardium. Of 177 test-operated embryos, 134 developed until desired stages, whereas of 77 sham-operated embryos, 66 survived. Test- and sham-operated hearts were dissected and analyzed for gross morphology at E6 and E8 (Fig. 1D–K). Test-operated embryos exhibited several cardiac abnormalities, including a reduction in the size of the ventricular chamber. The degree of epicardial deficiency in test-operated hearts was determined by immunostaining for cytokeratin, an established marker for epithelia, including the epicardium (Virágh et al., 1993). Sham-operated E6 hearts exhibited a cytokeratin-positive epicardial sheet that enveloped the entire ventricle (Fig. 1L). In test-operated samples, a spectrum of epicardial deficiency was observed (Fig. 1M–O). Section immunohistochemistry for cytokeratin further confirmed that the test-operated hearts lacked an intact epicardial covering (Fig. 1P–S). Subsequent experiments were conducted on test-operated samples that displayed the greatest degree of epicardial inhibition, as judged by histology and cytokeratin immunostaining, with sham-operated hearts as controls.

Cell Density in Epicardium-Deficient Hearts

As previously reported (Männer, 1993; Gittenberger-de Groot et al., 2000), delayed growth or thinning of the ventricular myocardium, both free wall and septal components, was evident in histologic sections of hearts lacking an epicardium at E6 and E8 (Fig. 2). The thickness of the ventricular compact zone was compared between epicardium-deficient hearts and sham controls. The myocardial thickness was expressed as a ratio of the area of the ventricular myocardial compact zone to the length of the outer perimeter of the ventricular myocardium, thus giving an index for the average thickness of the entire myocardial compact layer. Sham-operated hearts at E6 gave an index for myocardial thickness of 37 μm, whereas epicardium-deficient hearts displayed an index of 21 μm (Fig. 2I),

representing a 43% decrease in compact zone thickness. At E8, sham-operated hearts gave an index of 36 μm, whereas epicardium-deficient hearts had an index of 25 μm, a reduction of 31% compared with controls.

Cell density in the compact myocardium of epicardium-deficient and sham-operated hearts was quantified (Fig. 2J). Between E6 and E8, in control hearts there was an overall increase of 80% in cell density in the compact zone of the ventricular myocardium. At E6, cell density was approximately 9,900 cells/mm^2 in epicardium-deficient hearts, compared with approximately 9,000 cells/mm^2 in controls. Thus, the average cell density in the compact layer of the ventricular myocardium in epicardium-deficient hearts was approximately 10% higher than that of sham-operated hearts. At E8, the cell density in the compact layer of epicardium-deficient hearts was almost 20% higher than in control hearts (19,000 cells/mm^2 and 16,000 cells/mm^2, respectively). Therefore, the higher myocardial cell density in epicardium-deficient hearts may contribute, in part, to the reduced thickness of the compact zone.

Apoptosis in Epicardium-Deficient Hearts

Myocytes rarely undergo apoptotic death during development, except for those in the outflow tract and atrioventricular junction (Manasek, 1969b; Pexieder, 1975; Cheng et al., 2002). However, it is unknown whether myocyte survival in the compact myocardium depends upon the presence of the epicardium. To address this issue, apoptosis in the myocardium was examined in epicardium-deficient hearts by using the terminal deoxynucleotidyl transferase-mediated biotinylated UTP nick end labeling (TUNEL) assay. At E6, in sham-operated hearts approximately 0.08% of cells in the ventricular myocardial compact zone were TUNEL-positive (Fig. 3). In epicardium-deficient hearts at E6, however, 0.25% cells in the compact zone were TUNEL-positive, representing more than a threefold increase. At E8, the proportion of TUNEL-positive cells in sham-operated hearts was 1.2%, compared with 2.7% in epicardium-deficient hearts (Fig. 3), representing more than a twofold increase. Thus, epicardium-deficient hearts displayed an increase in the rate of apoptosis compared with controls. However, given that, in the absence of the epicardium, the proportion of cells undergoing apoptosis is still less than 3% of the total number of cells in the myocardium, it seems unlikely that this level of apoptosis could significantly contribute toward the pronounced reduction (31% by E6 and 43% by E8, Fig. 2) in the thickness of the myocardium seen in epicardium-deficient hearts.

Myocyte Proliferation in Epicardium-Deficient Hearts

Active proliferation of myocytes in the compact myocardium is the major mechanism of myocardial growth during early heart development (Manasek, 1968; Jeter and Cameron, 1971; Tokuyasu, 1990; Thompson et al., 1995). To examine the potential role of the epicardium in the regulation of myocyte proliferation, individual myocytes of the compact myocardium were tagged with a replication-defective, β-galactosidase (β-gal) -expressing retrovirus, CXL, at E3 (Fig. 4A) and the rate of production of clonally related, β-gal+ daughter myocytes was compared between control and epicardium-deficient hearts over a period of four days. In both experimental groups, β-gal+ myocyte clones formed as clusters within the myocardium (Fig. 4B–G). The number of myocytes in individual β-gal+ clusters of E7 hearts was then counted by using serial histologic sections (Fig. 4D,G). In control hearts, 49 cells were generated on average from individual parental myocytes between E3 and E7 (Fig. 4H), consistent with previous reports by us and others (Mikawa et al., 1992a; Mima et al., 1995; Lin et al., 2000; Hatcher et al., 2001). In epicardium-deficient, E7 hearts, β-gal+ clusters contained 29 cells on average, demonstrating a decrease of 41% in myocyte clone size (Fig. 4H). Thus, in the four days between injection at E3 and dissection at E7, myocytes in control hearts completed almost six cell cycles (the number of cell cycles required to produce 49 cells from a single progenitor cell), whereas those in epicardium-deficient hearts underwent less than five cell cycles. The overall loss of one cell cycle results in generation of 50% less cells in the myocardium. This loss of one cycle, together with an increased cell density, over the course of four days, therefore, is sufficient to account for the reduction (31% by E6 and 43% by E8, Fig. 2) in the thickness of the compact myocardium observed in epicardium-deficient hearts.

Transmural Pattern of Myocyte Proliferation Is Maintained in Epicardium-Deficient Hearts

Although the above data demonstrate that the rate of growth of myocyte clones declines in the absence of the epicardium, these data do not provide sufficient spatial information to examine transmural patterns of myocyte proliferation across the myocardium. To visualize this finding, control and epicardium-deficient hearts were exposed to bromodeoxyuridine (BrdU) for 4 hr at E6 and E8 before harvesting and the distribution of myocytes in S-phase of the cell cycle across the myocardium was analyzed (Fig. 5). In control hearts, more BrdU-positive cells were found in the compact myocardium than in the trabecular myocardium (Fig. 5A–D). In comparison, epicardium-deficient hearts displayed the same pattern of BrdU incorporation. In control hearts, at E6, 42% of cells were positive for BrdU incorporation in the compact zone, whereas epicardium-deficient hearts displayed a slightly smaller proportion (37%) of BrdU-positive cells (Fig. 5E). At E8, the proportion of BrdU-positive cells was 10% and 8% in control and epicardium-deficient hearts, respectively. Thus, the results suggest that the transmural gradient of myocardial proliferation occurs independently of signals from the epicardium.

Expression of FGF Ligands and FGF Receptor-1 in Epicardium-Deficient Hearts

The maintenance of a transmural gradient of myocyte proliferation in

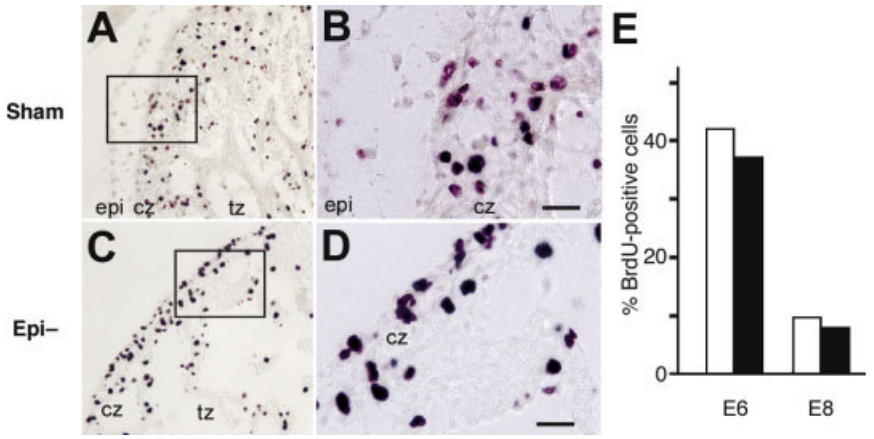

Fig. 5. The transmural pattern of myocyte proliferation is maintained in epicardium-deficient hearts. **A:** Section of a sham-operated heart at embryonic day (E) 6 showing bromodeoxyuridine (BrdU) -positive cells in the myocardium of the right ventricular wall. Note the higher proportion of BrdU-positive cells in the outer, compact myocardium relative to the inner, trabecular myocardium. **B:** Higher magnification of the boxed area in A. **C:** Section of an epicardium-deficient heart at E6 showing BrdU incorporation. A higher proportion of BrdU-positive cells in the compact myocardium is maintained. **D:** Higher magnification of the boxed area in C. **E:** Analysis of the number of BrdU-positive cells in the myocardium of sham-operated hearts (white bars) and epicardium-deficient hearts (black bars) at E6 (sham-operated, standard deviation from the mean (SDM), 10.1; epicardium-deficient, SDM, 10.5) and E8 (sham-operated, SDM, 2.68; epicardium-deficient, SDM, 3.45). cz, myocardial compact zone; tz, myocardial trabecular zone; epi, epicardium. Scale bars = 20 μm in B and D.

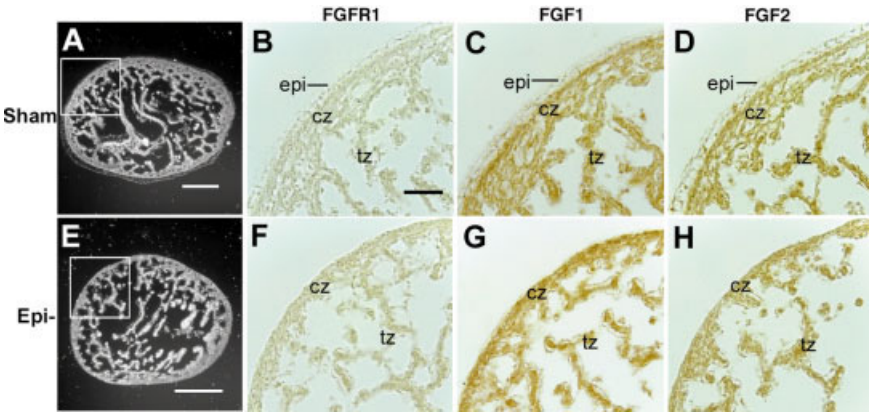

Fig. 6. Fibroblast growth factor receptor (FGFR) -1 and FGF1 and FGF2 protein expression at embryonic day (E) 5 in the ventricular myocardium of epicardium-deficient hearts. **A–D:** Sections of a sham-operated heart at E5. **E–H:** Sections of an epicardium-deficient heart at E5. A,E: Low-magnification, darkfield view of a sham-operated and an epicardium-deficient heart at E5, respectively. The boxed areas in A and E indicate the regions of nearby sections shown in B–D and F–H, respectively. B,F: FGFR-1 protein expression. C,G: FGF1 protein expression. D,H: FGF2 protein expression. cz, myocardial compact zone; tz, myocardial trabecular zone; epi, epicardium. Scale bars = 200 μm in A,E, 50 μm in B (applies to B–D, F–H).

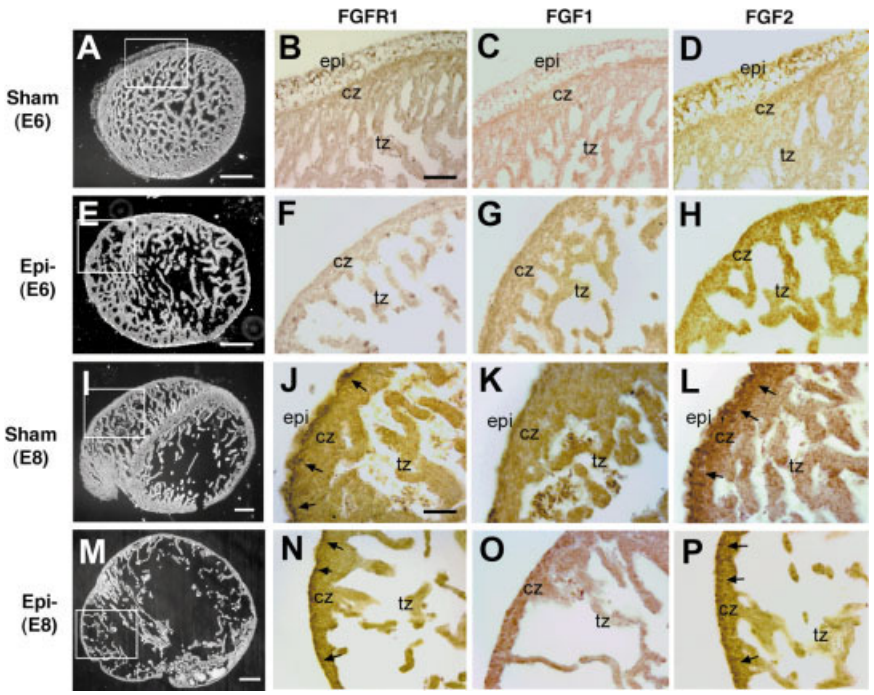

Fig. 7. Fibroblast growth factor receptor (FGFR) -1 and FGF1 and FGF2 protein expression at embryonic day (E) 6 and E8 in the ventricular myocardium of epicardium-deficient hearts. Sections of a sham-operated heart at E6 (A–D) and at E8 (I–L). Sections of an epicardium-deficient heart at E6 (E–H) and at E8 (M–P). **A,E,I,M:** Low-magnification, darkfield views of sections. The boxed areas indicate the regions of nearby sections shown in B–D, F–H, J–L, and N–P, respectively. **B,F,J,N:** FGFR-1 protein expression. **C,G,K,O:** FGF1 protein expression. **D,H,L,P:** FGF2 protein expression. Similar transmural expression patterns were observed in both the left and right ventricle. Arrows indicate regions of higher protein expression in the compact myocardium. cz, myocardial compact zone; tz, myocardial trabecular zone; epi, epicardium. Scale bars = 200μm in A,E,I,M, 50 μm in B (also applies to C,D,F–H), 50 μm in J (also applies to K,L,N–P).

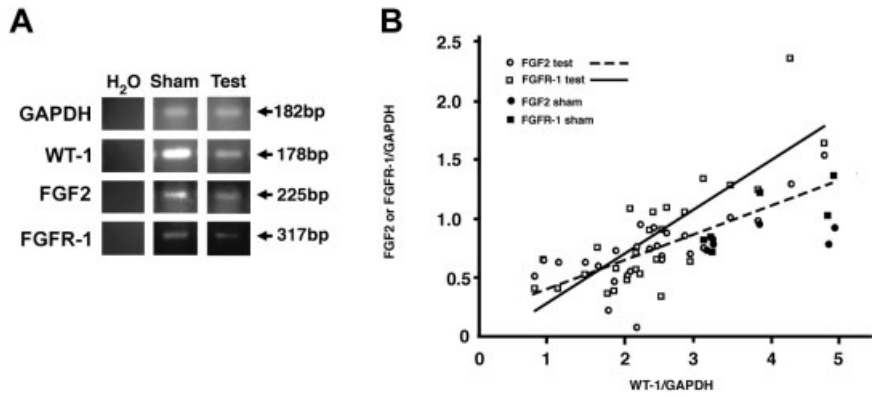

Fig. 8. Fibroblast growth factor-2 (FGF2) and FGF receptor (FGFR) -1 mRNA expression levels diminish in the ventricle of test-operated hearts concomitant with a reduction in WT-1 mRNA levels. **A:** Examples of reverse transcriptase-polymerase chain reaction amplicons, including a sham-operated control (Sham) and a test-operated sample (Test) that displayed a reduced level of WT-1 expression. The size of DNA fragments is indicated in base pairs (bp). H_2O, water control. **B:** The level of FGF2 and FGFR-1 expression for test-operated and sham control hearts plotted against the respective WT-1 value. As the WT-1 expression level declines in test-operated hearts, so too do the levels of FGF2 and FGFR-1. Circles, FGF2 values; squares, FGFR-1 values; filled circles and squares, sham control hearts; open circles and squares, test-operated hearts. Lines of best fit for test-operated hearts are shown: dashed line, FGF2 values; solid line, FGFR-1 values. R2 value for FGF2 expression in test-operated samples, 0.55; R2 value for FGFR1 expression in test-operated samples, 0.65. GAPDH, glyceraldehyde-3-phophate dehydrogenase.

epicardium-deficient hearts strongly suggested that the epicardium may not be essential for the expression patterns of mitogenic factors that induce and maintain the transmural pattern of myocyte proliferation in the embryonic hearts. To clarify this, the expression patterns of two major myocyte mitogenic factors, FGF-1 and FGF-2, and their major receptor, FGFR-1, were examined at various stages of development after inhibition of PE outgrowth. At E5, in sham-operated controls, FGFR-1, FGF1, and FGF2 proteins were detected throughout the compact and trabeculated myocardium (Fig. 6A–D). Epicardium-deficient hearts showed a similar distribution of these mitogenic factors throughout the myocardium compared with sham-operated controls (Fig. 6E–H). At E6, similar staining patterns of FGFR-1, FGF1, and FGF2 were obtained from both sham-operated control and epicardium-deficient hearts (Fig. 7A–H). At E8, stronger signals of FGFR-1 and FGF2 were detected in the outermost region of the compact zone in control hearts. Again, similar transmural patterns of immunostaining were detected in epicardium-deficient hearts (Fig. 7M–P). These results demonstrate that key components of FGF signaling, essential for myocyte proliferation, are expressed in the absence of the epicardium and that their transmural patterns of expression are maintained.

Levels of FGF2 and FGFR-1 Expression in Epicardium-Deficient Hearts

Although no significant alteration in the transmural pattern of FGF signaling components was detectable in the developing myocardium in the absence of the epicardium, it remained unclear whether the levels of these mitogenic factors were maintained in epicardium-deficient hearts. Because FGF signaling is a major factor in myocyte proliferation (Mikawa, 1995; Mima et al., 1995; Gisselbrecht et al., 1996; Ciruna et al., 1997; Sheikh et al., 1997, 1999; Michelson et al., 1998), a decrease in this expression could account for the reduced rate of myocyte proliferation observed in epicardium-deficient hearts. Therefore, we analyzed the levels of FGF2 and its major receptor, FGFR-1, in the ventricle of test-operated and sham-operated hearts at E7 by using reverse transcriptase-polymerase chain reaction (RT-PCR). Although in the above analyses, we specifically analyzed hearts that exhibited successful depletion of epicardium formation, it was difficult, if not impossible, to determine the level of epicardial inhibition at the time of dissection and before RNA isolation. Therefore, to gauge the levels of epicardial contribution in test-operated hearts, we analyzed the levels of WT-1 expression, a marker of proepicardial, epicardial, and subepicardial cells (Carmona et al., 2001; Pérez-Pomares et al., 2002). Figure 8A shows examples of RT-PCR amplicons for glyderaldehyde-3-phosphate dehydrogenase (GAPDH), WT-1, FGF2, and FGFR-1, of control and test-operated samples. In no case were amplicons detected in RT-negative (data not shown) or H_2O controls. The relative mRNA expression levels were calculated for test-operated and control samples, and FGF2 and FGFR-1 mRNA levels for each sample were then compared with WT-1 expression levels (Fig. 8B).

Whereas control samples displayed similar levels of WT-1 expression, test-operated samples demonstrated a range of expression levels. The latter is consistent with the range of depletion of the epicardium observed after microsurgical inhibition of PE outgrowth, as evaluated by cytokeratin immunostaining (see Fig. 1). Whereas FGF2 and FGFR-1 mRNA expression levels showed little variation between control samples, a range of levels was again observed in test-operated samples. The expression levels of both FGF2 and FGFR-1 mRNA in test samples showed a positive correlation with the corresponding WT-1 expression levels, suggesting that the expression of this mitogen and its major receptor are dependent on the extent of epicardium formation.

We have demonstrated that the epicardium is required for maintenance of mitogenic factors at the appropriate levels in the myocardium but that the myocardium is capable of establishing and maintaining a transmural pattern of these mitogenic factors in an epicardium-independent manner. These results strongly support the hypothesis that, in the absence of the epicardium,

the myocardium is capable of establishing a transmural axis, with an outer, compact region and an inner trabecular zone, as well as gradients of mitogenic factor expression and myocyte proliferation.

DISCUSSION

Establishing a transmural pattern across the myocardium is essential for proper heart development. A component of this axis is compartmentalization of the myocardium, with an outer, compact zone and an inner trabecular zone during development. Despite its importance for heart development, little is known about mechanisms that induce and maintain this patterning. The present study tested whether transmural patterning of the myocardium is dependent or independent of the adjacent epicardium or epicardium-derived cells.

In the embryonic heart, myocytes undergoing the greatest rate of proliferation are those in the compact layer, adjacent to the epicardium (Jeter and Cameron, 1971; Tokuyasu, 1990; Thompson et al., 1995). Although the epicardium is constantly present, the rate of myocyte proliferation diminishes as embryogenesis proceeds and ceases in the postnatal period (Jeter and Cameron, 1971), with postnatal growth of the myocardium achieved by hypertrophy rather than hyperplasia. FGFR-mediated signaling has been shown to be the major mitogenic cue for myocyte proliferation both in vertebrates and invertebrates (Mikawa, 1995; Mima et al., 1995; Gisselbrecht et al., 1996; Ciruna et al., 1997; Sheikh et al., 1997, 1999; Michelson et al., 1998). The expression of FGF ligands and receptors declines as embryos develop (Kardami and Fandrich, 1989; Consigli and Joseph-Silverstein, 1991; Patstone et al., 1993). Importantly, an age-dependent change in mitotic indices of the myocardium follows the change in expression of FGF ligands and receptors. Our immunohistochemical analysis of these major myocyte mitogenic factors demonstrated that the expression patterns of these factors are not significantly altered in epicardium-deficient hearts. Taken together, these data strongly suggest that the basic patterning of expression of FGF receptor and ligands across the myocardium occurs independently of the presence of the epicardium or epicardium-derived cells. Other mitogenic factors, such as NT3, trk-C (Lin et al., 2000), and TBX5 (Hatcher et al., 2001) are known to be involved in the regulation of myocyte proliferation in the embryonic heart. It remains to be seen whether these mitogenic factors are regulated by the epicardium.

This study also strongly suggests that compartmentalization of the myocardium is unaffected in epicardium-deficient hearts: the compact myocardium forms, albeit reduced in thickness, and trabeculae are apparent at all stages examined. This finding is unsurprising, because trabeculae form at a relatively early stage, before envelopment of the myocardium by the epicardium (for review, see Sedmera et al., 2000). Furthermore, trabecular formation is thought to be primarily patterned by signals from the endocardium rather than the epicardium (Corfas et al., 1995; Meyer and Birchmeier, 1995; Kramer et al., 1996; Ford et al., 1999). Nevertheless, this study confirms that the epicardium is not essential for maintenance of the trabecular myocardium, at least until E8.

Thinning of the compact myocardium is a common phenotype seen in several animal models in which epicardium formation is defective (Kreidberg et al., 1993; Kastner et al., 1994; Sucov et al., 1994; Kwee et al., 1995; Yang et al., 1995; Moore et al., 1999; Gittenberger-de Groot et al., 2000). However, it is unclear whether formation of a thinner myocardium in all models results from the same mechanism in all cases. There are several possible mechanisms that can give rise to a thinner myocardium, including myocyte hypotrophy, hypoplasia, and increased apoptosis. The present study demonstrated that these cell biological changes are induced in epicardium-deficient chick hearts. Consistent with this, several roles of retinoic acid derived from the epicardium (and mediated by RXRα) in the regulation of myocardium development have been postulated (Kastner et al., 1994; Sucov et al., 1994; Drysdale et al., 1997; Wobus et al., 1997; Aránega et al., 1999). However, a study on RXRβ null embryos, that display abnormally thin ventricular myocardial walls, used BrdU incorporation assays but failed to detect a difference in the mitotic index of cells in the compact myocardium (Kastner et al., 1994). Recent studies have implicated retinoic acid and/or erythropoietin in the secretion of a trophic factor from the epicardium that may be responsible for maintaining myocyte proliferation (Chen et al., 2002; Stuckmann et al., 2003). However, such a factor remains to be identified.

Although small differences in mitotic rates may not be easily detected by BrdU incorporation assays, our analysis of myocyte clonal growth successfully detected the loss of only one cell cycle between E3 and E7 in epicardium-deficient hearts. The loss of one cell cycle and a 10–20% increase in the density of myocytes are sufficient to account for the ~40% decrease in myocardial thickness induced in four days in epicardium-deficient hearts. Thus, our results provide clear evidence demonstrating that such subtle changes in these two cell biological events can give rise to severe morphogenetic phenotypes during early heart development.

The increase in cell density in the compact myocardium of epicardium-deficient hearts may be the result of several mechanisms. These include the possibility that there is premature maturation of myocytes in the compact zone, resulting in precocious development of trabeculae and further compaction of myocytes in the outer myocardial layer (as has been suggested by Kastner et al., 1997). Alternatively, the increased cell density may be the result of the lack of coronary vascular cells. These possibilities remain to be clarified.

In addition to the effects on myocyte proliferation, the present study detected a two- to threefold increase in levels of apoptosis in the myocardium of epicardium-deficient hearts. As the proportion of cells undergoing apoptosis is less

than 3% of the total number of cells in the myocardium, it seems unlikely that apoptosis would significantly influence overall myocardium development. It does, however, remain a possibility that the epicardium provides or induces survival factors to the myocardium in a paracrine manner. It has been shown, for example, that FGF2 can inhibit apoptosis in the ventricular myocardium (Zhao and Rivkees, 2000). Alternatively, the increased rate of cardiac myocyte cell death may be secondary to some other dysmorphogenesis or biophysical changes due to the thinning of myocardium.

In addition to the presence of the epicardium, there are various other proposed models for the establishment of gradients of growth factor expression and myocyte proliferation across the myocardium. These include a hypoxia model and a pressure-overloading model. Hypoxia has been postulated as a driving force in outer myocardial vascularization (where angioblasts from the epicardium delaminate and invade the myocardium), as the outermost myocardium of the developing heart is less well-supplied with blood than the trabeculated myocardium before the coronary vascular system is established (Yue and Tomanek, 1999; Sedmera et al., 2000). Although hypoxia is an inductive cue for the expression of vascular endothelial growth factor (VEGF; Stone et al., 1995; Tomanek et al., 1999b), no evidence has been shown to demonstrate that the expression of FGF ligands or receptors is hypoxia-dependent. Instead, FGF is a known inducer of VEGF (Seghezzi et al., 1998). It is, therefore, unlikely that hypoxia alone can regulate the transmural expression pattern of FGFs. Banding of the outflow tract in the embryonic chick heart to increase pressure load results in an initial increase in the size of the myocardium that is due to hyperplasia rather than hypertrophy (Clark et al., 1989). Such pressure overloading, which results in an increase in myocardial bulk by E6–E7, is accompanied by a concomitant increase in coronary vessel formation (Tomanek et al., 1999a). It is, however, unknown whether any myocyte mitogens are induced in the myocardium of pressure-overloaded hearts. However, FGF serves not only as a myocyte mitogen but also as a promoting factor for coronary vasculogenesis in vivo (Mikawa, 1995; Tomanek et al., 1998; Hyer et al., 1999) and in vitro (Ratajska et al., 1995). It remains to be seen whether these physicochemical factors play a role in patterning the expression of FGF ligands and/or receptors across the embryonic myocardium, thereby regulating myocyte proliferation.

We have used a nongenetic approach to produce epicardium-deficient hearts in the chick embryo to study the role of the epicardium in myocardial patterning and development. Previous studies have indicated that epicardial signaling may be required for proper myocardial development. Here, we demonstrate the necessity of the epicardium for myocytes to achieve proper rates of cell division. Consistent with this, FGF2 and FGFR-1 mRNA levels were reduced in epicardium-deficient hearts, and this reduction was proportional to the extent of epicardium deficiency. However, RT-PCR data alone is not sufficient to determine whether there are concomitant changes in FGF and FGFR protein expression levels, and so future Western blot analyses will be performed to clarify this point. Despite the importance of the epicardium in establishing the correct number of myocytes in the compact myocardium, we have also shown that the myocardium is capable of establishing morphogenetic gradients and patterns of protein expression necessary for heart development independently of the presence of the epicardium.

The role of the epicardium in myocardial patterning has remained unclear. We have begun to clarify this role by identifying mechanisms that occur independently of the epicardium (transmural patterning of the myocardium) and those that require the epicardium (the regulation of mitogen expression and myocyte proliferation). These findings highlight the importance of cell biological processes in myocardial growth and patterning that are mediated by epicardium-dependent and -independent mechanisms, thus providing a framework for future identification of other factors essential to myocardial development and furthering our understanding of myocyte biology.

EXPERIMENTAL PROCEDURES

Surgical Manipulations

Fertile chick eggs were purchased from either SPAFAS (Charles River, NJ) or Truslow Farms (Chestertown, MD). Fertilized chicken eggs were incubated at 38°C under humidified conditions. Embryos were staged according to the number of days of incubation or by the staging system (HH) of Hamburger and Hamilton (1951). Surgical inhibition of PE outgrowth was performed according to a method previously described (Männer, 1993) with slight modifications. Briefly, a small window was made in the egg with iris scissors and the pericardial cavity opened by tearing extraembryonic membranes with fine forceps. A small, rectangular piece of shell membrane was inserted into the pericardial cavity between the dorsal wall of the tubular heart and the PE, at HH stages 16–17, before their contact. Sham-operated embryos underwent the same procedure but had the shell membrane removed immediately. After surgical manipulations, eggs were sealed with Parafilm and returned to a humidified incubator to allow development to continue. Hearts were dissected for analysis at various stages of development (E5, E6, E7, and E8). Embryonic hearts destined for section analyses were fixed in 2% paraformaldehyde (PFA) in phosphate buffered saline (PBS) at 4°C for 2–4 hr, dehydrated in an ethanol series, cleared in CitriSolv (Fisher Scientific, Fair Lawn, NJ), and embedded in paraffin. Serial, 10-μm, transverse sections were cut and mounted on Superfrost slides (VWR, Chicago, IL).

Whole-Mount Immunostaining

Hearts were dissected from embryos, rinsed in PBS, fixed in 2% PFA in PBS for 2–4 hr at 4°C and washed in PBS. Endogenous peroxidase activity was quenched with 0.06% H_2O_2 in

PBS for 2 hr at room temperature. The tissues were then washed four times in PBB (PBS with 0.05% BSA) and three times in PBS/NGS (15% normal goat serum in PBS) at room temperature. Samples were incubated with an anti-cytokeratin antibody (Biomedical Technologies, Inc., Stoughton, MA) diluted 1/150 in PBS/NGS for 1 hr at room temperature and washed six times with PBS/NGS. Post antibody washes were performed at room temperature before an overnight wash in PBS/NGS at 4°C. Samples were incubated with a secondary antibody (goat anti-rabbit IgG conjugated with horseradish peroxidase; Sigma, St. Louis, MO) diluted 1/500 in PBS/NGS for 1 hr at room temperature. Post antibody washes were performed as above before washing samples three times in PBB. The staining reaction was performed by incubating samples in 500 μg/ml diaminobenzidine (DAB) in PBS with 0.03% H_2O_2 for 10 min at room temperature. Stained samples were washed in PBT (PBS with 0.05% Tween 20), fixed in 2% PFA in PBS, rinsed in PBT, and photographed.

Section Immunostaining

The following primary antibodies were used for immunostaining histologic sections: anti-cytokeratin antibody (Biomedical Technologies, Inc.), anti-FGF1 antibody (catalog no. sc-1884, Santa Cruz Biotechnology, Inc., Santa Cruz, CA), anti-FGF2 antibody (catalog no. sc-79, Santa Cruz Biotechnology, Inc.), and anti-FGFR-1 (Flg) antibody (catalog no. sc-121, Santa Cruz Biotechnology, Inc.). Immunohistochemistry was performed by using standard techniques. For consistency, sections for all analyses were selected from the region of the heart located approximately one third of the way up the ventricles from the apex. Briefly, sections were dewaxed in CitriSolv (Fisher Scientific), rehydrated in an ethanol/H_2O series and washed in PBS. Endogenous peroxidase activity was quenched by treatment with 0.3% H_2O_2 in PBS. Slides were then rinsed four times in PBS before blocking sections with PBTB (0.1% Tween 20, 2% BSA in PBS) and incubating overnight at 4°C with the primary antibody diluted 1/200 in PBTB. Samples were rinsed three times in PBS, incubated 1 hr with a secondary antibody (either goat anti-rabbit IgG or rabbit anti-goat IgG conjugated with horseradish peroxidase, Sigma) diluted 1/500 in PBTB at temperature. After rinsing three times in PBS, samples were exposed to 500 μg/ml DAB and 0.003% H_2O_2, rinsed in PBS, dehydrated in an ethanol/H_2O series, rinsed in CitriSolv, and mounted with Permount (Fisher Scientific).

TUNEL Assay

An In Situ Cell Death Detection kit (Roche, Germany) was used on histologic sections, according to the manufacturer's specifications with the following modifications: omission of the proteinase K step, the TUNEL reaction at 37°C for 90 min, and the signal conversion at 37°C for 45 min. TUNEL assay was performed on one to two sections from each of at least three embryos per group. Quantitation of total cell number in the compact myocardium was performed using 4,6-diamidino-2-phenylindole (DAPI) nuclear staining according to standard techniques.

Detection of DNA Synthesis

The thymidine analogue BrdU (DAKO, Carpinteria, CA) was applied to the vitelline membrane (75 μg for E6 and 120 μg for E8 embryos) and embryos reincubated for 4 hr before dissection. BrdU immunostaining was performed on histologic sections by using standard techniques described elsewhere (Lin et al., 2000). BrdU incorporation analysis was performed on one to two sections from each of at least three embryos per group. Quantification of total cell number in the compact myocardium was performed by using DAPI nuclear staining according to standard techniques.

Myocyte Proliferation Assay

A replication-incompetent retrovirus expressing β-galactosidase, CXL (Mikawa et al., 1991), was pressure-injected in ovo into the myocardium of epicardium-deficient and sham-operated hearts at E3, as described previously (Mikawa et al., 1992a,b). At E7, hearts were dissected, fixed in 2% PFA (in PBS), and stained with X-gal. Samples were embedded, sectioned, and mounted in Permount (Fisher Scientific) as described above. Myocyte clone size was quantified by counting the number of nuclei in X-gal–positive clones under phase microscopy as previously described (Mikawa et al., 1992a; Mima et al., 1995).

Data Documentation and Analysis

Images were captured by using either a Digital Photo Camera (DKC-5000, Sony) or a Spot RT Slider (2.3.1, Diagnostic Instruments, Inc.) using Adobe Photoshop (version 7.0, Adobe Systems, Inc.) or Spot (version 3.2.6 Diagnostic Instruments, Inc.) software, respectively. Images were adjusted for color levels, brightness, and contrast, and figures were compiled by using Adobe Photoshop software (version 7.0, Adobe Systems, Inc.). NIH Image 1.62 software (National Institutes of Health, Baltimore, MD) was used to determine the area of the compact myocardial layer in heart sections. The compact myocardium was defined as the region between the epicardium and the lower limit of the trabeculae. Standard deviation from the mean was calculated for groups of quantitative data. Statistical significance was determined by using an unpaired Student's *t*-test.

RT-PCR Expression Analyses

The ventricular component of epicardium-deficient and sham-operated control hearts was dissected out at E7 and RNA was extracted with TRIzol reagent (Invitrogen, San Diego, CA), according to the manufacturer's specifications. cDNA was produced from total RNA and PCR amplification performed as previously described (Pennisi et al., 2000). The primer pairs used were as follows: for GAPDH, forward 5′-TCG GTG TGA ACG GAT TTG-3′, reverse 5′-ATT CTCGGC CTT GAC TGT-3′; for WT-1, forward 5′-CGG ACC CCC TAC AAC AGT GA-3′, reverse 5′-CTG GCA CTC GTC GGA CAT CT-3′; for

FGF2, forward 5′-AAC TGC AGC TTC AAG CAG AAG-3′, reverse 5′-CGG GCT TGT ACT GTC CAG TCC-3′; and for FGFR-1, forward 5′-TGA CGT GCA GAG CAT CAA C-3′, reverse 5′-GCA GCT TCT TCT CCA TCT T-3′. PCR samples (8 μl of the 30 μl) were electrophoresed on a 1.2% agarose gel and digital images captured by using a Fluor-S MultiImager (Bio-Rad, Richmond, VA). Relative levels of band intensity were quantified by using Multi-Analyst version 1.0.2 software (Bio-Rad). Values for WT-1, FGF2, and FGFR-1 were normalized with the respective GAPDH levels. Test-operated values were expressed as a percentage of mean sham-control values.

ACKNOWLEDGMENTS

We thank Lisa Forgione, Lydia Miroff, and Theresa Zagreda for excellent histology support and Patrick Nahirney for expert technical advice. We also thank Bettye Ridley and David Reese for critical reading of this manuscript. D.J.P. was supported, in part, by a Charles H. Revson Foundation Postdoctoral Fellowship.

REFERENCES

Aránega AE, Velez C, Prados J, Melguizo C, Marchal JA, Arena N, Alvarez L, Aránega A. 1999. Modulation of α-actin and α-actinin proteins in cardiomyocytes by retinoic acid during development. Cells Tissues Organs 164:82–89.

Carmona R, González-Iriarte M, Pérez-Pomares JM, Muñoz-Chápuli R. 2001. Localization of the Wilm's tumour protein WT1 in avian embryos. Cell Tissue Res 303:173–186.

Chen THP, Chang TC, Kang JO, Choudhary B, Makita T, Tran CM, Burch JBE, Eid H, Sucov HM. 2002. Epicardial induction of fetal cardiomyocyte proliferation via a retinoic acid-inducible trophic factor. Dev Biol 250:198–207.

Cheng G, Wessels A, Gourdie RG, Thompson RP. 2002. Spatiotemporal and tissue specific distribution of apoptosis in the developing chick heart. Dev Dyn 223:119–133.

Ciruna BG, Schwartz L, Harpal K, Yamaguchi TP, Rossant J. 1997. Chimeric analysis of fibroblast growth factor receptor-1 (Fgfr1) function: a role for FGFR1 in morphogenetic movement through the primitive streak. Development 124:2829–2841.

Clark EB, Hu N, Frommelt P, Vandekieft GK, Dummett JL, Tomanek RJ. 1989. Effect of increased pressure on ventricular growth in stage 21 chick embryos. Am J Physiol 257:H55–H61.

Consigli SA, Joseph-Silverstein J. 1991. Immunolocalization of basic fibroblast growth factor during chicken cardiac development. J Cell Physiol 146:379–385.

Corfas G, Rosen KM, Aratake H, Krauss R, Fischbach GD. 1995. Differential expression of ARIA isoforms in the rat brain. Neuron 14:103–115.

Cummins P. 1993. Fibroblast and transforming growth factor expression in the cardiac myocyte. Cardiovasc Res 27: 1150–1154.

Dettman RW, Denetclaw W Jr, Ordahl CP, Bristow J. 1998. Common epicardial origin of coronary vascular smooth muscle, perivascular fibroblasts, and intermyocardial fibroblasts in the avian heart. Dev Biol 193:169–181.

Drysdale TA, Patterson KD, Saha M, Krieg PA. 1997. Retinoic acid can block differentiation of the myocardium after heart specification. Dev Biol 188:205–215.

Fishman MC, Chien KR. 1997. Fashioning the vertebrate heart: earliest embryonic decisions. Development 124:2099–2117.

Ford BD, Loeb JA, Fischbach GD. 1999. Neuregulin stimulates DNA synthesis in embryonic chick heart cells. Dev Biol 214:139–150.

Gassmann M, Casagranda F, Orioli D, Simon H, Lai C, Klein R, Lemke G. 1995. Aberrant neural and cardiac development in mice lacking the ErbB4 neuregulin receptor. Nature 378:390–394.

Gisselbrecht S, Skeath JB, Doe CQ, Michelson AM. 1996. heartless encodes a fibroblast growth factor receptor (DFR1/DFGF-R2) involved in the directional migration of early mesodermal cells in the Drosophila embryo. Genes Dev 10:3003–3017.

Gittenberger-de Groot AC, Vrancken Peeters MP, Bergwerff M, Mentink MM, Poelmann RE. 2000. Epicardial outgrowth inhibition leads to compensatory mesothelial outflow tract collar and abnormal cardiac septation and coronary formation. Circ Res 87:969–971.

Hamburger V, Hamilton HL. 1951. A series of normal stages in the development of the chick embryo. J Morphol 88:49–92.

Hatcher CJ, Kim MS, Mah CS, Goldstein MM, Wong B, Mikawa T, Basson CT. 2001. TBX5 transcription factor regulates cell proliferation during cardiogenesis. Dev Biol 230:177–188.

Hiruma T, Hirakow R. 1989. Epicardial formation in embryonic chick heart: computer-aided reconstruction, scanning, and transmission electron microscopic studies. Am J Anat 184:129–138.

Ho E, Shimada Y. 1978. Formation of the epicardium studied with the scanning electron microscope. Dev Biol 66:579–585.

Hyer J, Johansen M, Prasad A, Wessels A, Kirby ML, Gourdie RG, Mikawa T. 1999. Induction of Purkinje fiber differentiation by coronary arterialization. Proc Natl Acad Sci U S A 96:13214–13218.

Jeter JR Jr, Cameron IL. 1971. Cell proliferation patterns during cytodifferentiation in embryonic chick tissues: liver, heart and erythrocytes. J Embryol Exp Morphol 25:405–422.

Kardami E, Fandrich RR. 1989. Basic fibroblast growth factor in atria and ventricles of the vertebrate heart. J Cell Biol 109:1865–1875.

Kastner P, Grondona JM, Mark M, Gansmuller A, LeMeur M, Decimo D, Vonesch JL, Dollé P, Chambon P. 1994. Genetic analysis of RXR α developmental function: convergence of RXR and RAR signaling pathways in heart and eye morphogenesis. Cell 78:987–1003.

Kastner P, Messaddeq N, Mark M, Wendling O, Grondona JM, Ward S, Ghyselinck N, Chambon P. 1997. Vitamin A deficiency and mutations of RXRα, RXRβ, and RAR α lead to early differentiation of embryonic ventricular cardiomyocytes. Development 124:4749–4758.

Kirby ML. 1999. Contribution of neural crest to heart and vessel morphology. In: Harvey RP, Rosenthal N, editors. Heart development. San Diego: Academic Press. p 179–193.

Kramer R, Bucay N, Kane DJ, Martin LE, Tarpley JE, Theill LE. 1996. Neuregulins with an Ig-like domain are essential for mouse myocardial and neuronal development. Proc Natl Acad Sci U S A 93:4833–4838.

Kreidberg JA, Sariola H, Loring JM, Maeda M, Pelletier J, Housman D, Jaenisch R. 1993. WT-1 is required for early kidney development. Cell 74:679–691.

Kwee L, Baldwin HS, Shen HM, Stewart CL, Buck C, Buck CA, Labow MA. 1995. Defective development of the embryonic and extraembryonic circulatory systems in vascular cell adhesion molecule (VCAM-1) deficient mice. Development 121:489–503.

Lee KF, Simon H, Chen H, Bates B, Hung MC, Hauser C. 1995. Requirement for neuregulin receptor erbB2 in neural and cardiac development. Nature 378: 394–398.

Li WE, Waldo K, Linask KL, Chen T, Wessels A, Parmacek MS, Kirby ML, Lo CW. 2002. An essential role for connexin43 gap junctions in mouse coronary artery development. Development 129:2031–2042.

Lin MI, Das I, Schwartz GM, Tsoulfas P, Mikawa T, Hempstead BL. 2000. Trk C receptor signaling regulates cardiac myocyte proliferation during early heart development in vivo. Dev Biol 226: 180–191.

Manasek FJ. 1968. Embryonic development of the heart. I. A light and electron microscopic study of myocardial development in the early chick embryo. J Morphol 125:329–365.

Manasek FJ. 1969a. Embryonic development of the heart. II. Formation of the

epicardium. J Embryol Exp Morphol 22: 333–348.
Manasek FJ. 1969b. Myocardial cell death in the embryonic chick ventricle. J Embryol Exp Morphol 21:271–284.
Männer J. 1993. Experimental study on the formation of the epicardium in chick embryos. Anat Embryol (Berl) 187: 281–289.
Männer J. 2000. Cardiac looping in the chick embryo: a morphological review with special reference to terminological and biomechanical aspects of the looping process. Anat Rec 259:248–262.
Meyer D, Birchmeier C. 1995. Multiple essential functions of neuregulin in development. Nature 378:386–390.
Michelson AM, Gisselbrecht S, Zhou Y, Baek KH, Buff EM. 1998. Dual functions of the heartless fibroblast growth factor receptor in development of the Drosophila embryonic mesoderm. Dev Genet 22:212–229.
Mikawa T. 1995. Retroviral targeting of FGF and FGFR in cardiomyocytes and coronary vascular cells during heart development. Ann N Y Acad Sci 752: 506–516.
Mikawa T, Fischman DA. 1992. Retroviral analysis of cardiac morphogenesis: discontinuous formation of coronary vessels. Proc Natl Acad Sci U S A 89:9504–9508.
Mikawa T, Gourdie RG. 1996. Pericardial mesoderm generates a population of coronary smooth muscle cells migrating into the heart along with ingrowth of the epicardial organ. Dev Biol 174: 221–232.
Mikawa T, Fischman DA, Dougherty JP, Brown AM. 1991. In vivo analysis of a new *lacZ* retrovirus vector suitable for cell lineage marking in avian and other species. Exp Cell Res 195:516–523.
Mikawa T, Borisov A, Brown AM, Fischman DA. 1992a. Clonal analysis of cardiac morphogenesis in the chicken embryo using a replication-defective retrovirus. I. Formation of the ventricular myocardium. Dev Dyn 193:11–23.
Mikawa T, Cohen-Gould L, Fischman DA. 1992b. Clonal analysis of cardiac morphogenesis in the chicken embryo using a replication-defective retrovirus. III. Polyclonal origin of adjacent ventricular myocytes. Dev Dyn 195:133–141.
Mima T, Ueno H, Fischman DA, Williams LT, Mikawa T. 1995. Fibroblast growth factor receptor is required for in vivo cardiac myocyte proliferation at early embryonic stages of heart development. Proc Natl Acad Sci U S A 92:467–471.
Moore AW, McInnes L, Kreidberg J, Hastie ND, Schedl A. 1999. YAC complementation shows a requirement for *Wt1* in the development of epicardium, adrenal gland and throughout nephrogenesis. Development 126:1845–1857.
Patstone G, Pasquale EB, Maher PA. 1993. Different members of the fibroblast growth factor receptor family are specific to distinct cell types in the developing chicken embryo. Dev Biol 155: 107–123.
Pennisi D, Bowles J, Nagy A, Muscat G, Koopman P. 2000. Mice null for *Sox18* are viable and display a mild coat defect. Mol Cell Biol 20:9331–9336.
Pérez-Pomares JM, Macías D, García-Garrido L, Muñoz-Chápuli R. 1998. The origin of the subepicardial mesenchyme in the avian embryo: an immunohistochemical and quail-chick chimera study. Dev Biol 200:57–68.
Pérez-Pomares JM, Phelps A, Sedmerova M, Carmona R, González-Iriarte M, Muñoz-Chápuli R, Wessels A. 2002. Experimental studies on the spatiotemporal expression of WT1 and RALDH2 in the embryonic avian heart: a model for the regulation of myocardial and valvuloseptal development by epicardially derived cells (EPDCs). Dev Biol 247: 307–326.
Pexieder T. 1975. Cell death in the morphogenesis and teratogenesis of the heart. Adv Anat Embryol Cell Biol 51:3–99.
Ratajska A, Torry RJ, Kitten GT, Kolker SJ, Tomanek RJ. 1995. Modulation of cell migration and vessel formation by vascular endothelial growth factor and basic fibroblast growth factor in cultured embryonic heart. Dev Dyn 203: 399–407.
Rychter Z, Ostádal B. 1971. Fate of "sinusoidal" intertrabecular spaces of the cardiac wall after development of the coronary vascular bed in chick embryo. Folia Morphol 19:31–44.
Rychterova V. 1971. Principle of growth in thickness of the heart ventricular wall in the chick embryo. Folia Morphol 19:262–272.
Sedmera D, Pexieder T, Vuillemin M, Thompson RP, Anderson RH. 2000. Developmental patterning of the myocardium. Anat Rec 258:319–337.
Seghezzi G, Patel S, Ren CJ, Gualandris A, Pintucci G, Robbins ES, Shapiro RL, Galloway AC, Rifkin DB, Mignatti P. 1998. Fibroblast growth factor-2 (FGF-2) induces vascular endothelial growth factor (VEGF) expression in the endothelial cells of forming capillaries: an autocrine mechanism contributing to angiogenesis. J Cell Biol 141:1659–1673.
Sheikh F, Jin Y, Pasumarthi KB, Kardami E, Cattini PA. 1997. Expression of fibroblast growth factor receptor-1 in rat heart H9c2 myoblasts increases cell proliferation. Mol Cell Biochem 176:89–97.
Sheikh F, Fandrich RR, Kardami E, Cattini PA. 1999. Overexpression of long or short FGFR-1 results in FGF-2-mediated proliferation in neonatal cardiac myocyte cultures. Cardiovasc Res 42:696–705.
Stone J, Itin A, Alon T, Pe'er J, Gnessin H, Chan-Ling T, Keshet E. 1995. Development of retinal vasculature is mediated by hypoxia-induced vascular endothelial growth factor (VEGF) expression by neuroglia. J Neurosci 15:4738–4747.
Stuckmann I, Evans S, Lassar AB. 2003. Erythropoietin and retinoic acid, secreted from the epicardium, are required for cardiac myocyte proliferation. Dev Biol 255:334–349.
Sucov HM, Dyson E, Gumeringer CL, Price J, Chien KR, Evans RM. 1994. RXRα mutant mice establish a genetic basis for vitamin A signaling in heart morphogenesis. Genes Dev 8:1007–1018.
Thompson RP, Kanai T, Germroth PG, Gourdie RG, Thomas PS, Barton PJR, Mikawa T, Anderson RH. 1995. Organization and function of early specialized myocardium. In: Clark EB, Markwald RR, Takao A, editors. Developmental mechanisms of congenital heart disease. Armonk: Futura. p 269–279.
Tokuyasu KT. 1990. Co-development of embryonic myocardium and myocardial circulation. In: Clark EB, Takao A, editors. Developmental cardiology: morphogenesis and function. New York: Futura. p 205–218.
Tomanek RJ, Lotun K, Clark EB, Suvarna PR, Hu N. 1998. VEGF and bFGF stimulate myocardial vascularization in embryonic chick. Am J Physiol 274:H1620–H1626.
Tomanek RJ, Hu N, Phan B, Clark EB. 1999a. Rate of coronary vascularization during embryonic chicken development is influenced by the rate of myocardial growth. Cardiovasc Res 41: 663–671.
Tomanek RJ, Ratajska A, Kitten GT, Yue X, Sandra A. 1999b. Vascular endothelial growth factor expression coincides with coronary vasculogenesis and angiogenesis. Dev Dyn 215:54–61.
Virágh S, Challice CE. 1981. The origin of the epicardium and the embryonic myocardial circulation in the mouse. Anat Rec 201:157–168.
Virágh S, Gittenberger-de Groot AC, Poelmann RE, Kálmán F. 1993. Early development of quail heart epicardium and associated vascular and glandular structures. Anat Embryol (Berl) 188: 381–393.
Wilson JG, Warkany J. 1949. Aortic-arch and cardiac anomalies in the offspring of vitamin A-deficient rats. Am J Anat 85:113–155.
Wobus AM, Kaomei G, Shan J, Wellner MC, Rohwedel J, Guanju J, Fleischmann B, Katus HA, Hescheler J, Franz WM. 1997. Retinoic acid accelerates embryonic stem cell-derived cardiac differentiation and enhances development of ventricular cardiomyocytes. J Mol Cell Cardiol 29:1525–1539.
Yang JT, Rayburn H, Hynes RO. 1995. Cell adhesion events mediated by α_4 integrins are essential in placental and cardiac development. Development 121: 549–560.
Yue X, Tomanek RJ. 1999. Stimulation of coronary vasculogenesis/angiogenesis by hypoxia in cultured embryonic hearts. Dev Dyn 216:28–36.
Zhao Z, Rivkees SA. 2000. Programmed cell death in the developing heart: regulation by BMP4 and FGF2. Dev Dyn 217:388–400.